Publications

2005

Transient Non-linear Heat Conduction Solution by a Dual Reciprocity Boundary Element Method with an Effective Posteriori Error Estimator

Eduardo Divo
Embry-Riddle Aeronautical University, Eduardo.divo@erau.edu

Alain J. Kassab
University of Central Florida, Alain.Kassab@ucf.edu

Transient Non-linear Heat Conduction Solution by a Dual Reciprocity Boundary Element Method with an Effective Posteriori Error Estimator

Eduardo Divo [1], Alain J. Kassab [2]

Abstract: A Dual Reciprocity Boundary Element Method is formulated to solve non-linear heat conduction problems. The approach is based on using the Kirchhoff transform along with lagging of the effective non-linear thermal diffusivity. A posteriori error estimate is used to provide effective estimates of the temporal and spatial error. A numerical example is used to demonstrate the approach.

1 Introduction

Several numerical techniques have been proposed to generate boundary integral representations for the diffusion equation. The first such formulation, derived by Rizzo and Shippy (Rizzo and Shippy, 1970), applied Laplace transforms to produce a time-independent boundary integral equation in the transform domain. This equation is then solved for a sequence of values of the transform parameter and a numerical transform inversion is employed to compute the physical variables in the real space. Chang et al. (Chang, Kang and Chen, 1973) and Shaw (Shaw, 1974) employed the time-dependent fundamental solution given by Morse and Feshbach (Morse and Feshbach, 1953) and Carslaw and Jaeger (Carslaw and Jaeger, 1959), among others, to derive BEM formulations over space and time. The formulation was later extended by Wrobel and Brebbia (Wrobel and Brebbia, 1979) to allow higher-order space and time interpolation functions to be included, thus making the analysis of practical engineering problems possible. Another technique is the dual reciprocity boundary element method (DRBEM), initially applied to transient heat conduction problems by Wrobel et al. (Wrobel, Brebbia and Nardini, 1986), which interprets the time derivative in the diffusion equation as a body force and employs the fundamental solution to Laplace's equation to generate a

boundary integral equation. Alternative boundary integral formulations include replacing the time derivative in the diffusion equation by a finite difference approximation, as proposed by Curran et al. (Curran, Cross and Lewis, 1980), and the multiple reciprocity formulation of Nowak (Nowak, 1987). The boundary element method and the dual reciprocity method are discussed in detail in several monographs (Brebbia, 1978) and recent reviews of advances in BEM can be found in Kassab and Wrobel (Kassab and Wrobel, 2000) and Kassab et al. (Kassab, Wrobel, Bialecki and Divo, 2004).

In this paper, we present the details of a formulation of the dual reciprocity boundary element method for transient non-linear heat conduction. We formulate the problem using the classical Kirchhoff transform defining a new dependent variable. The transient governing equation remains nonlinear. The non-linearity is removed from the spatial operator and appears confined to a non-linear effective thermal diffusivity. We follow standard BEM procedure to convert this differential equation to a boundary integral equation and to finally arrive at the time-marching DRBEM equations. The non-linearity of the problem is addressed by lagging or extrapolating the coefficients of a diagonal matrix multiplying the elements of the capacitance matrix. As such, this approach to non-linear heat transfer modeling by the DRBEM is efficient in that it only requires a diagonal matrix multiplication to update the capacitance matrix at each iteration updating the temperature and heat flux to the new time level. We solve the problem in 3D using constant elements and standard conic radial basis functions (Powell, 1992), both to be defined later in the paper. We also develop an effective posteriori error estimator, and we implement this estimator for the transient case and for constant elements. In this approach, the values of the temperatures at the corners of each constant 3D element are computed by a distance weighted extrapolation of the four closest constant element nodes. Subsequently, a bilinear interpolation of the corner values for each element

[1] Engineering Technology Department, University of Central Florida, Orlando, Florida 32816-2450

[2] Mechanical, Materials, and Aerospace Engineering Department, University of Central Florida, Orlando, Florida 32816-2450

provides a higher order estimate of the temperature at the center of each constant element. This higher order curve fit prediction of the constant element solution is compared at each constant element node with the value predicted by the constant DRBEM code, and a root mean square error is estimated at each time level. A transient non-linear example is solved for validation, and results indicate that the proposed error estimator is very effective in bounding the error and following the trend of the global error as a function of time. This error estimator is readily extended to any higher order discontinuous BEM discretization.

2   Dual Reciprocity Boundary Element Method for Linear Heat Conduction

We first develop the dual reciprocity boundary element formulation for the solution of linear transient heat conduction in solids, then extend the approach to non-linear heat conduction. The linear problem is governed by the diffusion equation

$$\nabla \cdot [k\nabla T] = \rho c_p \frac{\partial T}{\partial t} \tag{1}$$

where t is time, T is temperature, k is the thermal conductivity (here taken as a function of temperature), ρ is the density, and c_p is the specific heat. The problem definition is completed with the specification of boundary conditions

$$\begin{aligned} T(\Gamma,t) &= \widehat{T}(\Gamma,t) \\ q(\Gamma,t) &= \widehat{q}(\Gamma,t) \\ q(\Gamma,t) &= h[T(\Gamma,t) - T_\infty] \end{aligned} \tag{2}$$

and initial condition, $T(x,t_0) = T_0(x)$. Here, $q(x,t)$ is the outward-facing normal heat flux, $q(x,t) = -k\partial T/\partial n$, and x denotes spatial coordinate(s) depending on the dimensionality of the problem.

In the DRBEM formulation (Brebbia and Partridge, 1992), the right-hand-side of the diffusion equation, Eqn. (1), is first expanded as,

$$\rho c_p \frac{\partial T(x,t)}{\partial t} = \sum_{k=1}^{N+L} \alpha_k(t) f_k(x) \tag{3}$$

where N is the number of BEM boundary nodes at which dual reciprocity points are collocated, L is the number

of additional internal dual reciprocity (DR) collocation points. The expansion functions are chosen to satisfy

$$f_k(x) = \nabla \cdot [k\nabla u_k(x)] \tag{4}$$

Once the DR expansion function f_k is chosen, then the functions u_k are readily derived by solving Eqn. (4) in the appropriate dimension. This will be discussed later.
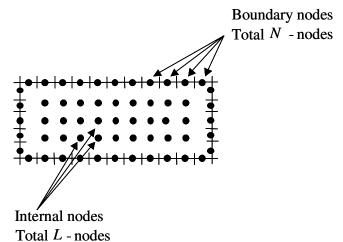

Figure 1 : Two-dimensional example of a constant element DRBEM discretization: N-boundary points corresponding to constant element nodes and L-internal points.

Substitution of Eqn. (4) and Eqn. (3) into Eqn. (1) leads to,

$$\nabla \cdot [k\nabla T(x,t)] = \sum_{k=1}^{N+L} \alpha_k(t) \nabla \cdot [k\nabla u_k(x)] \tag{5}$$

We consider a three-dimensional problem. Consequently, we multiply both sides of the above by the 3-D fundamental solution to the Laplace equation,

$$T^*(x,\xi) = \frac{1}{4\pi k\, r(x,\xi)} \tag{6}$$

where $r(x,\xi)$ is the radial distance between the field point x and the source point ξ. Integrating over the domain, applying Green's first identity twice to both sides of the above equation leads to the following integral equation, for any location of the source point ξ inside the domain
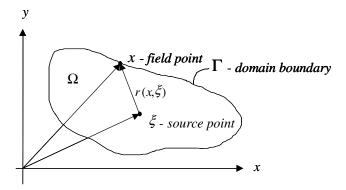
Figure 2 : Illustration of the domain Ω bounded by the boundary Γ, the field point x, the source point ξ, and the $r(x,\xi)$ is the radial distance between the field point and the source point.

boundary Γ,

$$T(\xi,t) + \oint_\Gamma \left[q(x,t)\, T^*(x,\xi) - F(x,\xi)\, T(x,t) \right] d\Gamma$$

$$= \sum_{k=1}^{N+L} \alpha_k(t) \left\{ u_k(\xi) \right.$$

$$\left. + \oint_\Gamma \left[p_k(x)\, T^*(x,\xi) - F(x,\xi)\, u_k(x) \right] d\Gamma \right\} \qquad (7)$$

where the following notation is used:

$$\begin{aligned}
q(x,t) &= -k\nabla T(x,t)\cdot\widehat{n} \\
p_k(x) &= -k\nabla u_k(x)\cdot\widehat{n} \\
F(x,\xi) &= -k\nabla T^*(x,\xi)\cdot\widehat{n}
\end{aligned} \qquad (8)$$

where the outward-drawn normal to the boundary Γ is denoted by $\widehat{n}$. In arriving at the above integral equations, it is recognized that the free-space solution $T^*(x,\xi)$ to the Laplace equation satisfies (precisely why it was chosen as the test function in the first place),

$$\nabla \cdot [k\nabla T^*(x,\xi)] = -\delta(x,\xi) \qquad (9)$$

where $\delta(x,\xi)$ is the Dirac delta function. The domain integrals are eliminated using the sifting property of the Dirac delta function to give:

$$\int_\Omega \nabla \cdot [k\nabla T^*(x,\xi)]\, T(x,t)\, d\Omega = -T(\xi,t)$$

$$\int_\Omega \nabla \cdot [k\nabla T^*(x,\xi)]\, u_k(x)\, d\Omega = -u_k(\xi) \qquad (10)$$

When the point ξ lies on the boundary, then a limiting procedure can be used to arrive at the following boundary integral equation

$$C(\xi)\, T(\xi,t) + \oint_\Gamma \left[q(x,t)\, T^*(x,\xi) - F(x,\xi)\, T(x,t) \right] d\Gamma$$

$$= \sum_{k=1}^{N+L} \alpha_k(t) \left\{ C(\xi)\, u_k(\xi) \right.$$

$$\left. + \oint_\Gamma \left[p_k(x)\, T^*(x,\xi) - F(x,\xi)\, u_k(x) \right] d\Gamma \right\} \qquad (11)$$

where the surface integrals over the boundary Γ are taken in their Cauchy Principal Value (CPV) and the free term $C(\xi)$ can be shown analytically to be

$$C(\xi) = \oint_\Gamma -k\nabla T^*(x,\xi)\cdot\widehat{n}\, d\Gamma \qquad (12)$$

and it is equal to 1/2 when the source point lies on a smooth boundary. Thus, Eqn. (11) can be considered a general equation that is valid both at the boundary and at the interior with $C(\xi) = 1/2$ when $\xi \in \Gamma$ and $C(\xi) = 1$ when $\xi \in \Omega$. A pattern of $j = 1,2...N$ boundary nodes is introduced on the boundary, the boundary is discretized piecewise as

$$\Gamma = \sum_{j=1}^{N} \Delta\Gamma_j \qquad (13)$$

Although higher order elements are used for better accuracy in practice, we will use a constant element discretization exclusively in this work. In this element, the geometry is modeled using bilinear shape functions, while the temperature and flux are modeled as piecewise constant over each boundary element. Figure 3 below shows a typical constant boundary element along with its transformed representation in the local $\eta - \zeta$ coordinate system.
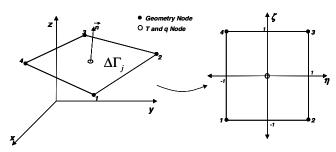

Figure 3 : Constant boundary element.

Notice that the geometric nodal locations of the element are ordered counterclockwise such that the normal vector always points outwards from the domain of the problem. The global coordinate system (x, y, z) is transformed into a local coordinate system (η, ζ) using bi-linear shape functions. The temperature and heat flux are modeled as constant with the node located at the geometric center of the boundary element, thus

$$T(\eta, \zeta, t) = T_j(t) \text{ and } q(\eta, \zeta, t) = q_j(t)$$
$$\text{on } \Delta\Gamma_j \tag{14}$$

Collocating Eqn. (11) by taking the source point ξ at the $i = 1, 2 ... N + L$ boundary and interior DR nodes leads to

$$C_i T_i(t) - \sum_{j=1}^{N} \widehat{H}_{ij} T_j(t) + \sum_{j=1}^{N} G_{ij} q_j(t)$$
$$= \sum_{k=1}^{N+L} \alpha_k(t) \left\{ C_i u_k(x_i) - \sum_{j=1}^{N} \widehat{H}_{ij} u_k(x_j) + \sum_{j=1}^{N} G_{ij} p_k(x_j) \right\} \tag{15}$$

for $i = 1, 2, ... N + L$, leading to the matrix equation

$$\underset{=}{G} \underset{\sim}{q} - \underset{=}{H} \underset{\sim}{T} = \left\{ \underset{=}{G}\underset{=}{P} - \underset{=}{H}\underset{=}{U} \right\} \underset{\sim}{\alpha} \tag{16}$$

The influence coefficients $\widehat{H}_{ij}$ and G_{ij} that are elements of the matrices $\underset{=}{G}$ and $\underset{=}{H}$ are defined as integrals over the boundary element $\Delta\Gamma_j$,

$$\widehat{H}_{ij} = \iint_{\Delta\Gamma_j} F(x, \xi_i) \, d\Gamma$$
$$G_{ij} = \iint_{\Delta\Gamma_j} T^*(x, \xi_i) \, d\Gamma \tag{17}$$

and these are evaluated using adaptive quadratures based on Gauss-Legendre rules (Kassab, Wrobel, Bialecki and Divo, 2004).

At this point it is instructive to describe the DR expansion functions $f_k(x)$ and the derived functions $u_k(x)$ and $p_k(x)$ in order to explain how the matrices $\underset{=}{P}$ and $\underset{=}{U}$ are evaluated. We use exclusively the radially symmetric conic RBF (Powell, 1992),

$$f_k(x) = 1 + r_k(x) \tag{18}$$

where $r_k(x)$ is the radial distance from the DR collocation point k, in 3-D,

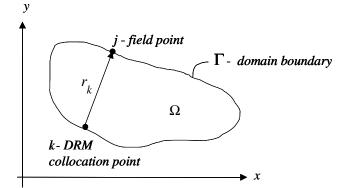$$r_k(x) = \sqrt{(x - x_k)^2 + (y - y_k)^2 + (z - z_k)^2} \tag{19}$$

Figure 4 : Illustration of radial distance r_k used in conic RBFs.

From this definition, the $u_k(x)$ function is derived from the relation

$$1 + r_k = \frac{1}{r_k^2} \frac{\partial}{\partial r_k} \left(k r_k^2 \frac{\partial u_k}{\partial r_k} \right) \tag{20}$$

which is readily integrated to give

$$u_k(x) = \frac{1}{k} \left[\frac{r_k^3(x)}{12} + \frac{r_k^2(x)}{6} \right] \tag{21}$$

The function $p_k(x)$ is derived from its definition, Eqn. (8), as

$$p_k(x) = -\left(\frac{r_k(x)}{4} + \frac{1}{3} \right) [(x - x_k)n_x + (y - y_k)n_y + (z - z_k)n_z] \tag{22}$$

where, n_x, n_y, and n_z are the x-, y-, and z- components of the outward-drawn normal of each boundary element. The result that

$$\frac{\partial r_k}{\partial x} = \frac{(x - x_k)}{r_k}, \frac{\partial r_k}{\partial y} = \frac{(y - y_k)}{r_k}, \text{ and } \frac{\partial r_k}{\partial z} = \frac{(z - z_k)}{r_k} \tag{23}$$

has also been used in deriving $p_k(x)$. The matrices $\underset{=}{U}$ and $\underset{=}{P}$ are obtained by evaluating the expansion functions u_k and its normal derivatives p_k at every dual reciprocity point respectively. The k-th column of the interpolating matrices $\underset{=}{U}$ and $\underset{=}{P}$ is then seen to be comprised of the vectors $\underset{\sim}{u}_k$ of values of $U_{j,k} = u_k(x_j)$ and $\underset{\sim}{p}_k$ of values of $P_{j,k} = p_k(x_j)$ with j= 1, 2 ... N + L.

Collocating Eqn. (3) and Eqn. (4) at the $N + L$ dual reciprocity expansion points leads to the linear system of equations,

$$\rho c_p \underset{\sim}{\dot{T}} = \underset{=}{F} \underset{\sim}{\alpha} \tag{24}$$

The notation $\underset{\sim}{\dot{T}}$ has been used to represent the vector of values of the partial derivative of the temperature at the j$= 1, 2 ... N + L$ boundary and dual reciprocity points. The interpolating matrix $\underset{=}{F}$ has a structure with each k-th column of the matrix comprised of the vector $\underset{\sim k}{f}$ of values of $F_{j,k} = f_k(x_j)$ with j$= 1, 2, ... N + L$. Inverting the interpolating matrix $\underset{=}{F}$ to solve explicitly for the vector of expansion coefficients $\underset{\sim}{\alpha}$, allows Eqn. (16) to be recast as

$$\underset{=}{H}\underset{\sim}{T} - \underset{=}{G}\underset{\sim}{q} = \underset{=}{C}\underset{\sim}{\dot{T}} \tag{25}$$

where, $\underset{\sim}{\dot{T}}$ is the vector of time derivatives of the nodal temperatures and the capacitance matrix $\underset{=}{C}$ is given by

$$\underset{=}{C} = -\rho c_p \left\{ \underset{==}{G}\underset{=}{P} - \underset{==}{H}\underset{=}{U} \right\} \underset{=}{F}^{-1} \tag{26}$$

The final step in DRBEM for the diffusion equation involves the finite differencing of the temporal derivative in Eqn. (25), and the approximation of the nodal temperatures and fluxes. Applying a first order finite difference in time, and using parameters θ_T and θ_q to position the temperature vector, $\underset{\sim}{T}$, and the flux vector, $\underset{\sim}{q}$, between the time steps p and $p + 1$,

$$T(t) = (1 - \theta_T)T^p + \theta_T T^{p+1}$$
$$q(t) = (1 - \theta_q)q^p + \theta_q q^{p+1}$$
$$\dot{T}(t) = \frac{T^{p+1} - T^p}{\Delta t} \tag{27}$$

yields the final form of the DRBEM equations,

$$\left(\Delta t \, \theta_T \, \underset{=}{H} - \underset{=}{C} \right) \underset{\sim}{T}^{p+1} - \left(\Delta t \, \theta_q \, \underset{=}{G} \right) \underset{\sim}{q}^{p+1}$$
$$= \left[\Delta t \, (\theta_T - 1) \, \underset{=}{H} - \underset{=}{C} \right] \underset{\sim}{T}^p + \Delta t \, (1 - \theta_q) \underset{=}{G}\underset{\sim}{q}^p \tag{28}$$

where the right-hand-side of Eqn. (28) is known from the previous time step p and Δt is the time step taken.

Upon introduction of the boundary conditions, Eqn. (28) is solved for the temperature evolution. The choice of the parameters θ_T and θ_q dictate the order of the method in time. We use the fully-implicit option, setting θ_T and θ_q equal to one. The resulting system of linear equations is solved using LU decomposition. Hence, if the time step is held constant, the LU factors are computed only once, and, thereafter, only a forward and backward substitution is needed to solve the linear system at every time step.

This completes the description of the linear conduction solution. Attention is now given to the non-linear formulation. The Kirchhoff transform is introduced, and the DRBEM development of the linear case is naturally extended to the nonlinear case.

3 DRBEM for Non-Linear Heat Conduction

The governing equation under consideration is the transient heat conduction equation with temperature-dependent thermal conductivity and specific heat as,

$$\nabla \cdot [k(T)\nabla T] = \rho c_p(T) \frac{\partial T}{\partial t} \tag{29}$$

Here, the thermophysical properties are taken as temperature dependent. The classical Kirchhoff transform (özisik, 1986) can be used to transform the governing equation prior to solving the resulting transformed equation by standard BEM. This is described by several authors for steady state problems, see Bialecki and Nowak (Bialecki and Nowak, 1981), Azevedo and Wrobel (Azevedo and Wrobel, 1988), and Bialecki and Nahlik (Bialecki and Nhalik, 1989). A new dependent variable is defined as,

$$J(T) = \frac{1}{k_o} \int_{T_o}^{T} k(T) dT \tag{30}$$

where T_o is a reference temperature at which the reference thermal conductivity k_o is evaluated. The Kirchhoff transform is the area under the $k(T)$ curve and as such is a monotonic single-valued function of temperature. The integral can be evaluated analytically or numerically via a quadrature and the curve of J vs. T can readily be constructed. This curve can be made a subroutine or statement function that can be called at any time a temperature is required when operating in the Kirchhoff transform domain. The Kirchhoff transformation defines the dependent variable $J(T)$ (with units of temperature) such

that, $k(T)dT = k_o dJ$, and consequently

$$k(T)\nabla T = k_o \nabla J$$
$$k(T)\partial T = k_o \partial J \tag{31}$$

Introducing these results into the governing heat conduction equation leads to the following equation in the Kirchhoff temperature

$$\nabla \cdot [k_o \nabla J] = \frac{k_o \rho c_p(T)}{k(T)} \frac{\partial J}{\partial t} \tag{32}$$

Imposed temperature and heat flux boundary conditions transform linearly to give:

$$\left. T \right|_{r_s} = \widehat{T}_s \quad \blacktriangleright \quad \left. J \right|_{r_s} = J(\widehat{T}_s)$$
$$-k \frac{\partial T}{\partial n}\Big|_{r_s} = \widehat{q}_s \quad \blacktriangleright \quad -k_o \frac{\partial J}{\partial n}\Big|_{r_s} = \widehat{q}_s \tag{33}$$

where r_s denotes a point on the surface. Consequently, the developments above apply directly to non-linear heat conduction with the Kirchhoff temperature as dependent variable. In the case of convective boundary conditions, the transformation is non-linear and an additional iteration must be used.

Defining the function

$$\beta(T) = \frac{k_o \rho c_p(T)}{k(T)} \tag{34}$$

the non-linear heat conduction equation becomes

$$\nabla \cdot [k_o \nabla J] = \beta(T) \frac{\partial J}{\partial t} \tag{35}$$

Comparing with the linear heat conduction equation, see Eqn. (1), it is clear that the DRBEM development for the linear case can be readily adopted by replacing all references to T by J, and by:

1. modifying the fundamental solution, see Eqn. (6), by replacing T^* by J^* and k by k_o as,

$$J^*(x,\xi) = \frac{1}{4\pi k_o\, r(x,\xi)} \tag{36}$$

2. modifying the definitions in Eqn. (8) to

$$q(x,t) = -k_o \nabla J(x,t) \cdot \widehat{n}$$
$$p_k(x) = -k_o \nabla u_k(x) \cdot \widehat{n}$$
$$F(x,\xi) = -k_o \nabla J^*(x,\xi) \cdot \widehat{n} \tag{37}$$

3. re-writing the DRBEM equations as

$$\underline{\underline{H}}\,\underline{J} - \underline{\underline{G}}\,\underline{q} = \underline{\underline{C}}\,\underline{\dot{J}} \tag{38}$$

where $\underline{\dot{J}}$ is the vector of time derivatives of the Kirchhoff temperatures at each node and with the capacitance matrix interpreted as,

$$\underline{\underline{C}} = -\left\{\underline{\underline{G}}\,\underline{\underline{P}} - \underline{\underline{H}}\,\underline{\underline{U}}\right\}\underline{\underline{F}}^{-1}\underline{\underline{\beta}} \tag{39}$$

with $\underline{\underline{\beta}}$ as a diagonal matrix given by

$$\underline{\underline{\beta}} = \begin{bmatrix} \beta(T_1) & 0 & 0 & 0 \\ 0 & \beta(T_2) & 0 & 0 \\ 0 & 0 & \ddots & 0 \\ 0 & 0 & 0 & \beta(T_{N+L}) \end{bmatrix} \tag{40}$$

where $\beta(T_j)$ is the function $\beta(T)$ evaluated at each of the DR nodes, $j = 1, 2 ... N + L$.

Finally, the DRBEM equations read for the Kirchhoff temperature:

$$\left(\Delta t\, \theta_t \underline{\underline{H}} - \underline{\underline{C}}\right) \underline{J}^{p+1} - \left(\Delta t\, \theta_q \underline{\underline{G}}\right) \underline{q}^{p+1}$$
$$= \left[\Delta t\,(\theta_t - 1)\,\underline{\underline{H}} - \underline{\underline{C}}\right]\underline{J}^p + \Delta t\,(1 - \theta_q)\underline{\underline{G}}\,\underline{q}^p \tag{41}$$

Here again Δt is the time step taken. The question remains how to evaluate the elements of the diagonal matrix $\underline{\underline{\beta}}$. Two alternatives can be followed:

1. lag the matrix in time, where each element is evaluated when solving Eqn. (41) at the time level $p + 1$ as:

$$\beta(T_j^{p+1}) \cong \beta(T_j^p) \tag{42}$$

where temperature T_j^p (is known from the unique J vs. T curve) evaluated at the at the point j at the previous time level p.

2. extrapolated from previous time levels, where each element is evaluated when solving Eqn. (41) at the time level $p + 1$ as:

$$\beta(T_j^{p+1}) \cong \beta(T_j^p) + \frac{d\beta(T)}{dT}\Big|_{T_j^p}\left(T_j^p - T_j^{p-1}\right) \tag{43}$$

where $\left.\frac{d\beta(T)}{dT}\right|_{T_j^p}$ is the derivative of $\beta(T)$ with respect to temperature (a known expression) evaluated at the temperature at the point j at the previous time level p.

The lagging approach may be used throughout the solution process, or may be used once at the first time step and subsequently, the extrapolation method may be used for all remaining time steps. This should provide a more accurate but computationally more burdensome approach. Results reported in this paper are obtained by lagging the coefficient $\beta(T)$.

4 Posteriori Error Estimator

An error estimation of the solution provided by the BEM is of crucial importance when dealing with numerically sensitive problems such as optimization, inverse, and control problems, where the BEM can be used as the field solver and where a statistical analysis of the error is necessary for regularization and control of the solution. There has been much work carried out to address this subject in particular with regards to mesh adaptation and refinement (Rencis and Kirk, 2003-Ingber and Mitra, 1992). In order to arrive at an efficient global posteriori error estimator that does not require multiple solutions, a strategy can be adopted consisting in generating a simulated a higher-order solution from a computed lower-order solution and comparing the simulated and the computed at the same locations. This idea is an extension of finite element error estimation procedures, adopted by Rencis et al. (Rencis and Kirk, 2003), to BEM applications.

In a typical three-dimensional transient BEM solution of the temperature field using bilinear sub parametric (constant) elements where the temperatures are retrieved as constant values along the element surface, $T_{c,j}$ (labeled by circles in Fig. 5), the values of the temperatures at the corner k of boundary element j, $T_{\text{corner},k,j}$, can be obtained by a distance-weighted interpolation of the nodal temperatures, $T_{c,i}$, of all elements i ($i = 1...NS$) sharing the corner k,

$$T_{\text{corner},k,j} = \frac{\sum_{i=1}^{NS} \frac{1}{r_i} T_{c,i}|_{i \in k}}{\sum_{i=1}^{NS} \frac{1}{r_i}|_{i \in k}} \tag{44}$$

where r_i are the distances from the corner to the neighboring element centers. The temperature field described by $T_{\text{corner},k,j}$ is a simulated higher-order (bilinear) field.

Furthermore, this high-order temperature distribution at corner nodes can be collapsed back to the constant boundary element node locations (centers) by a simple average:

$$T_{l,j} = \frac{1}{4} \sum_{k=1}^{4} T_{\text{corner},k,j} \tag{45}$$

An error estimate for the temperature at any boundary element node j is thus approximated, simply as the difference between the computed and interpolated solutions,

$$e_j = |T_{l,j} - T_{c,j}| \tag{46}$$

normalized over the maximum temperature difference. This is a very efficient posteriori error estimation as it only requires one computed solution, $T_{c,j}$, to approximate an error distribution that would otherwise require a higher-order (bilinear) BEM solution of the same problem.

5 Numerical Examples

A nonlinear verification example has been formulated in such a manner as to permit comparison with an analytical solution. Consider the nonlinear heat transfer problem in a rectangular parallelepiped, see Fig. 6. The thermophysical property variations with temperature are taken as

$$\begin{aligned} k(T) &= k_o e^{k_1(T-T_o)} \\ c_p(T) &= c_{po} + c_{p1} tanh[c_{p2}(T-T_o)] \end{aligned} \tag{47}$$

The initial condition is taken as uniform, $T(x,y,z,0) = \widehat{T}_0$. The boundary conditions are imposed as

$$\begin{aligned} T(x,y,0,t) &= \widehat{T}_o \\ -k(T)\nabla T \cdot \widehat{n} \Big|_{(x,y,L_z,t)} &= \widehat{q}_u \end{aligned} \tag{48}$$

and elsewhere on the barrel surface as insulated,

$$-k(T)\nabla T \cdot \widehat{n} = 0 \tag{49}$$

The properties are taken as those of stainless steel with

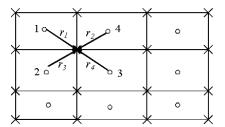$$\begin{aligned} c_{p0} &= 477\,J/kgK \\ c_{p1} &= 1235\,J/kgK \\ c_{p2} &= 3.94 \times 10^{-3}\,K^{-1} \\ \rho &= 7900\,kg/m^3 \\ k_o &= 14.9\,W/mK \\ k_1 &= 1.08\text{x}10^{-3}K^{-1} \end{aligned} \tag{50}$$

○   Constant boundary element node location, also location at
    which the extrapolated temperatures are linearly interpolated.

✕   Corner of constant boundary element location to which
    constant boundary element temperatures are extrapolated
    by distance weighted average.

(a) extrapolation of the constant element temperatures at the constant
     element nodal temperatures to the corner node locations.

(b) Linear interpolation of the temperature at the
constant boundary element node location j

Figure 5 : Illustration of the nomenclature for the global
a posteriori error estimator.

with these choices, we find that $\beta(T) = \frac{k_0}{k(T)}\rho c_p(T) \sim$ constant over the range of temperatures $300 - 400K$. Thus, the problem can be solved analytically in the Kirchhoff transform space as

$$J(T) = \sum_{n=0}^{\infty} \left[\frac{2q_u(-1)^n}{k_o\lambda_n^2 L_z} \right] sin(\lambda_n z) e^{-\frac{k_o\lambda_n^2}{\beta}t} \qquad (51)$$

where the eigenvalues are given by

$$\lambda_n = \frac{\pi}{2L_z}(2n+1) \qquad (52)$$

The temperature is obtained by inverting the Kirchhoff transform as described in the above section. The initial condition, dimensions of the problem and heat flux
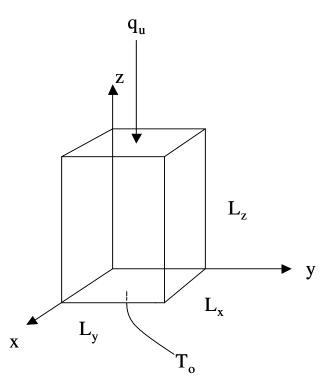

Figure 6 : Rectangular parallelepiped subjected to a constant temperature, T_o, at $z = 0$, a constant heat flux, q_u , at $z = L_z$, and insulated on all other surfaces.

are chosen to provide a solution with temperatures in the range $300 - 400K$ and are taken as:

$$L_x = L_y = L_z = 0.1m$$
$$\widehat{T}(x,y,z,0) = 300K$$
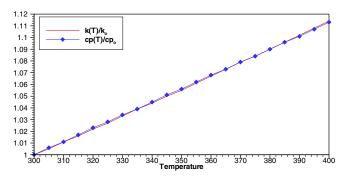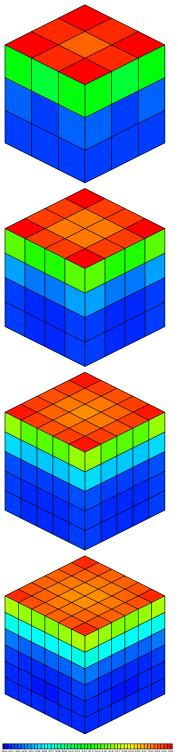$$\widehat{q}_u = -3000\,W/m^2 \qquad (53)$$

Figure 7 : Variation of the thermophysical properties for the example problem.

Figure 8 : Surface temperature distribution after 1 second predicted by the DRBEM using four different discretization levels.
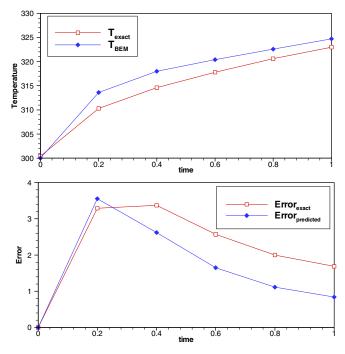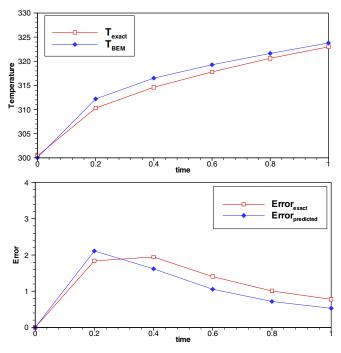

Figure 9 : Comparison of BEM and exact solutions and comparison of exact and predicted error for the 3 x 3 x 3 mesh configuration.

Figure 10 : Comparison of BEM and exact solutions and comparison of exact and predicted error for the 4 x 4 x 4 mesh configuration.

Figure 11 : Comparison of BEM and exact solutions and comparison of exact and predicted error for the 5 x 5 x 5 mesh configuration.

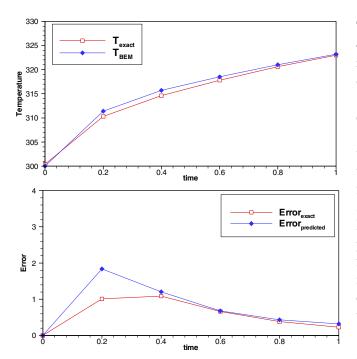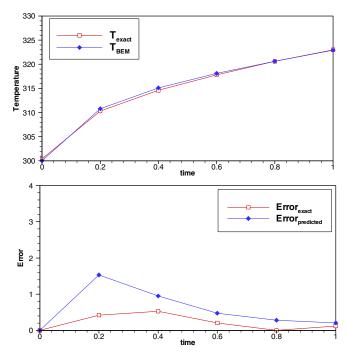**Figure 12** : Comparison of BEM and exact solutions and comparison of exact and predicted error for the 6 x 6 x 6 mesh configuration.

The transient conduction problem is solved in 3D using 4 levels of constant boundary element discretization corresponding to 3, 4, 5 and 6 boundary elements per edge of the block to demonstrate convergence of the numerical solution. The BEM discretizations for the four mesh levels along with the surface temperature distribution after 1 second are shown in figure 8. Figures 9 to 12 show the temperature evolution comparison from 0 to 1 second and the error estimation compared to the exact error for the four different BEM discretization levels. All error levels are reported in terms of absolute deviations between the BEM-computed and exact temperatures. The results are plotted for the upper wall at $z = L_z$ at the midpoint of that face. The results illustrate the efficacy of the error estimator. Convergence is demonstrated and the trend of the error estimator provides a conservative approximation to the exact error in temperature.

6   Conclusions

In this paper, we have reviewed the dual reciprocity boundary element method for linear diffusion and proposed an approach to solve non-linear diffusion problems. We have also provided an error estimator that is computationally inexpensive to evaluate. Numerical results provide confidence in the approach and indicate that the error estimator is able to predict the temporal trend of the exact error at different discretization levels.

References

Rizzo, F.J.; and Shippy, D.J. (1970): A Method of Solution for Certain Problems of Transient Heat Conduction, *AIAA Journal*, Vol. 8, No. 11, pp. 2004-2009.

Chang, Y.P.; Kang, C.S.; and Chen, D.J. (1973): The Use of Fundamental Green's Functions for the Solution of Problems of Heat Conduction in Anisotropic Media, *International Journal of Heat Mass Transfer*, Vol. 16, pp. 1905-1918.

Shaw, R.P. (1974): An Integral Equation Approach to Diffusion, *Int. J. Heat Mass Trans.*, Vol. 17, pp. 693-699.

Morse, P.M. and Feshbach, H. (1953): *Methods of Theoretical Physics, Part I and II*, McGraw Hill Book Co., New York.

Carslaw, H.S. and Jaeger, J.C. (1959): *Conduction of Heat in Solids*, 2nd ed., Clarendon Press, Oxford.

L.C. Wrobel and C.A. Brebbia (1979): *The Boundary Element Method for Steady-State and Transient Heat Conduction,* in R.W. Lewis and K. Morgan (eds.), Numerical Methods in Thermal Problems, Vol. 1, Pineridge Press, Swansea.

L.C. Wrobel, C.A. Brebbia, and D. Nardini (1986): *The Dual Reciprocity Boundary Element Formulation for Transient Heat Conduction, Finite Elements in Water Resources V.*, Computational Mechanics Publications, Southampton.

D. Curran, M. Cross and B.A. Lewis (1980): *A Preliminary Analysis of Boundary Element Methods applied to Parabolic Partial Differential Equations, New Developments in Boundary Element Methods*, Computational Mechanics Publications, C.A. Brebbia (ed.), Southampton, Computational Mechanics Publications.

A.J. Nowak (1987): *Solution of Transient Heat Conduction Problems using Boundary-Only Formulation*, in C.A. Brebbia, W.L. Wendland, and G. Kuhn (eds.), BEM IX, Vol. 3, Computational Mechanics Publications, Southampton and Springer-Verlag, Berlin.

C.A. Brebbia (1978): *The Boundary Element Method*, Pentech Press, London.

C.A. Brebbia, J.C.F, Telles, J.C.F. and L.C. Wrobel (1984): *Boundary Element Techniques*, Springer-Verlag, Berlin.

C.A. Brebbia and J.J. Dominguez (1989): *Boundary Elements: An Introductory Course, Computational Mechanics Pub.*, Southampton and McGraw-Hill, New York.

J.H. Kane (1993): *Boundary Element Analysis in Engineering Continuum Mechanics*, Prentice-Hall, New Jersey.

P.K., Banerjee (1994): *The Boundary Element Methods in Engineering*, McGraw Hill Book Co., New York.

L.C. Wrobel and M.A., Aliabadi (2002): *The Boundary Element Method*, Vol. 1 & 2, Wiley, New York.

E.A. Divo and A.J. Kassab (2003): *Boundary Element Method for Heat Conduction with Applications in Non-Homogeneous Media*, Wessex Institute of Technology Press, Southampton, UK, and Boston, USA.

C.A. Brebbia, P. Partridge, and L.C. Wrobel (1992): *The Dual Reciprocity Boundary Element Method*, Computational Mechanics and Elsevier Applied Science, Southampton, U.K.

A.J. Kassab and L.C. Wrobel (2000): *"Boundary Element Methods in Heat Conduction," Chapter 5 in Recent Advances in Numerical Heat Transfer*, W.J. Mincowycz and E. M. Sparrow, (eds.), Vol. 2, Taylor and Francis, New York, 2000, pp. 143-188.

A.J. Kassab, L.C. Wrobel, R. Bialecki, and E. Divo (2004): *Boundary Elements in Heat Transfer*," Chapter 6 in Handbook Of Numerical Heat Transfer, 2nd Edition, Minkowycz, W., Sparrow, E.M., and Murthy, J. Y. (eds.), John Wiley and Sons, 2004.

M.J.D. Powell (1992): *The Theory of Radial Basis Function Approximation, Advances in Numerical Analysis*, Vol. II, Light, W. (ed.), Oxford Science Publications, 1992.

N.M. Özisk (1980): *Heat Conduction*, John Wiley and Sons, New York.

R.A. Bialecki and A.J. Nowak (1981): Boundary Value Problems in Heat Conduction with Nonlinear Material and Nonlinear Boundary Conditions, *Applied Mathematical Modelling*, Vol. 5, pp. 417-421.

J.P.S. Azevedo and L.C., Wrobel (1988): Non-Linear Heat Conduction in Composite Bodies: A Boundary Element Formulation, *International Journal for Numerical Methods in Engineering*, Vol. 26, pp. 19-38.

R.A. Bialecki and R. Nhalik (1989): Solving Nonlinear Steady State Potential Problems in Inhomogeneous Bodies Using the Boundary Element Method, *Numerical Heat Transfer*, Part B, Vol. 15, pp. 79-96.

J.J. Rencis and R.A. Kirk (2003): *Local and Global Error Estimates for Three-Dimensional Heat Conduction Problems*, in Brebbia, C.A. and Dippery, R.E., (eds.), BETECH XV, Proc. of the 15th. Intl. Conf. on Boundary Element Technology, WIT Press, Boston, 321-329.

J.J. Rencis and K.Y. Jong (1989): A Self-Adaptive h-Refinement Technique for the Boundary Element Method, *Computer Methods in Applied Mechanics and Engineering*, Vol. 73, pp. 295-316, 1989.

M. Guiggiani (1990): Error Indicators for Adaptive Mesh Refinement in the Boundary Element Method-a new approach, *International Journal for Numerical Methods in Engineering*, Vol. 29, pp. 1247-1269.

M. Guggiani (1996): Sensitivity Analysis for Boundary Element Error Estimation and Mesh Refinement, *International Journal for Numerical Methods in Engineering*, Vol. 39, pp. 2907-2920.

M.S. Ingber and A.K. Mitra (1992): Grid Redistribution Based on Measurable Error Indicators for the Direct Boundary Element Method, *Engineering Analysis with Boundary Element*, Vol. 9, pp. 13-19.